

# $(\text{Bi,R})_2\text{O}_3$ (R: Nd, Sm and Dy) oxides as potential pigments

B. Gonzalvo<sup>a</sup>, J. Romero<sup>a</sup>, F. Fernández<sup>b</sup>, M.J. Torralvo<sup>a,\*</sup>

<sup>a</sup>Departamento de Química Inorgánica I, Facultad de Ciencias Químicas, Universidad Complutense de Madrid, 28040 Madrid, Spain

<sup>b</sup>Departamento Química Industrial y Polímeros, EUITI, Universidad Politécnica de Madrid, 28012 Madrid, Spain

## Abstract

In this work we have tackled the feasibility of the colored oxides in the  $\text{Bi}_2\text{O}_3\text{--R}_2\text{O}_3$  system as ecological inorganic pigments. We have prepared by solid state reaction the mixed oxides  $(\text{Bi}_2\text{O}_3)_{1-x}(\text{R}_2\text{O}_3)_x$ , R: Nd, Sm and Dy, with nominal compositions: Nd,  $x=0.2$  and  $0.5$ ; Sm,  $x=0.4$ ; and Dy,  $x=0.35$ . The obtained orange  $(\text{Bi}_2\text{O}_3)_{0.6}(\text{Sm}_2\text{O}_3)_{0.4}$  and  $(\text{Bi}_2\text{O}_3)_{0.65}(\text{Dy}_2\text{O}_3)_{0.35}$  oxides present f.c.c. fluorite-type structure.  $(\text{Bi}_2\text{O}_3)_{0.8}(\text{Nd}_2\text{O}_3)_{0.2}$  oxide consists of a mixture of two phases which present f.c.c.  $\delta\text{-Bi}_2\text{O}_3$  and Bi–Sr–O-type structures in the 900–1200°C temperature range. In the synthesis of the oxide with nominal composition  $(\text{Bi}_2\text{O}_3)_{0.5}(\text{Nd}_2\text{O}_3)_{0.5}$  we have obtained a greenish sample with higher neodymium content. This sample presents the  $\text{Bi}_3\text{R}_5\text{O}_{12}$ -type structure. Diffuse reflectance data and color coordinates suggest that the  $(\text{Bi}_2\text{O}_3)_{0.6}(\text{Sm}_2\text{O}_3)_{0.4}$  and  $(\text{Bi}_2\text{O}_3)_{0.65}(\text{Dy}_2\text{O}_3)_{0.35}$  oxides are expected to be promising candidates as new ecological pigments. © 2001 Elsevier Science B.V. All rights reserved.

**Keywords:** Bismuth–rare earth mixed oxides; Safe inorganic pigments; Optical properties

## 1. Introduction

The high temperature phase of bismuth sesquioxide  $\delta\text{-Bi}_2\text{O}_3$ , which is stable in the 730–825°C temperature range, has been intensively studied because of its high oxygen-ion conductivity [1]. The structure of the  $\delta$ -phase is based on a face centered cubic cation sublattice and can be described as a defective fluorite structure where 1/4 of the anion sites are vacant [2]. This high oxygen vacancy concentration gives rise to a high oxygen-ion mobility. The  $\delta$ -phase may be stabilized below room temperature by partial cationic substitution for  $\text{Bi}^{3+}$ . Thus, the use of  $\text{R}^{3+}$  cations (R: lanthanide or yttrium) has appeared effective though a variety of crystal phases have been observed depending on the kind and amount of the rare earth cation used and the synthesis conditions employed [3,4]. Recently, phase equilibrium studies of the  $\text{Bi}_{1-x}\text{R}_x\text{O}_{1.5}$  oxides (R: La–Er and Y) have revealed that the stabilized  $\delta$  phase is a metastable phase at room temperature [5–7].

The high-oxide-ion conduction observed in the mentioned  $\delta\text{-Bi}_2\text{O}_3$  has given rise to relevant work about the structural and electrical properties of  $\text{Bi}_2\text{O}_3$ -based solid

solutions, such as  $\text{Bi}_2\text{O}_3\text{--R}_2\text{O}_3$  systems, because of their potential use as electrolyte materials in solid-oxide fuel cells or as oxygen sensors. However, in this work we have tackled a different side of the  $\text{Bi}_2\text{O}_3\text{--R}_2\text{O}_3$  systems that, as far we know, has not been studied. This is the feasibility of these colored oxides as ecological inorganic pigments.

## 2. Experimental

Mixed oxides  $(\text{Bi}_2\text{O}_3)_{1-x}(\text{R}_2\text{O}_3)_x$ , R: Nd, Sm and Dy, with nominal compositions: Nd,  $x=0.2$  and  $0.5$ ; Sm,  $x=0.4$ ; and Dy,  $x=0.35$ , have been prepared. The synthesis of the samples was carried out in alumina crucibles from stoichiometric amounts of  $\text{Bi}_2\text{O}_3$  and  $\text{R}_2\text{O}_3$  oxides, which were mixed and annealed in air at different temperatures. The samples were firstly heated at 800°C during 48 h and then annealed each 50°C up to 1000°C (R: Sm and Dy) or 1200°C (R: Nd) during 48 h.  $\text{Bi}_2\text{O}_3$  was obtained by thermal decomposition of  $\text{Bi}(\text{NO}_3)_3 \cdot 5\text{H}_2\text{O}$  at 700°C and  $\text{R}_2\text{O}_3$  oxides were heated in air at 800°C during 8 h before use. The products were characterized by X-ray powder diffraction with a Philips X'Pert MPD diffractometer. X-ray diffraction patterns were recorded in the 10–120°  $2\theta$  range using Cu  $\text{K}\alpha$  radiation. Lattice parameters were obtained applying a least square refinement method and

\*Corresponding author. Tel.: +34-91-394-4343; fax: +34-91-394-4352.

E-mail address: torralvo@eucmos.sim.ucm.es (M.J. Torralvo).

using W powder as internal standard. Morphological analysis was performed by means of scanning electron microscopy, with a JEOL JSM-6400 electron microscope. Color measurements were made with a LUCI spectrometer operating in the 380–720-nm range. The instrument was calibrated using the BAM-waster standard LZM 128. The color coordinates have been determined according to the 1976 CIE LAB color scales (DIM 6174).

### 3. Results and discussion

X-ray diffraction patterns of  $(\text{Bi}_2\text{O}_3)_{0.6}(\text{Sm}_2\text{O}_3)_{0.4}$  and  $(\text{Bi}_2\text{O}_3)_{0.65}(\text{Dy}_2\text{O}_3)_{0.35}$  samples treated at 900°C (Fig. 1a) can be indexed in an f.c.c. fluorite-type cell. It is worth noting that the characteristic diffraction reflections of a fluorite-like structure are already present in the diffraction pattern of the dysprosium sample treated at 800°C. However, the samarium sample only shows these characteristic reflections after heating at 900°C. In both dysprosium and samarium samples, the f.c.c. fluorite structure is retained after 1000°C treatment. From semiquantitative EDS analyses we can deduce the  $(\text{Bi}_2\text{O}_3)_{0.59}(\text{Sm}_2\text{O}_3)_{0.41}$  and  $(\text{Bi}_2\text{O}_3)_{0.62}(\text{Dy}_2\text{O}_3)_{0.38}$  compositions, that agree with the nominal compositions. The calculated lattice parameters corresponding to the samples annealed at 900°C are shown in Table 1. In both cases, the results are in good agreement with those previously reported [4]. On the other hand, Fig. 2 shows the scanning micrographs corresponding to the samarium and dysprosium samples annealed at 900 and 1000°C. In both cases the particles are agglomerated and they are more heterogeneous in size for the  $(\text{Bi}_2\text{O}_3)_{0.65}(\text{Dy}_2\text{O}_3)_{0.35}$  sample. When the annealing temperature increases, the particles grow as a result of the beginning of the sinterization (Fig. 2c and d).

In the  $\text{Bi}_2\text{O}_3\text{--Nd}_2\text{O}_3$  system, samples with nominal composition  $(\text{Bi}_2\text{O}_3)_{0.8}(\text{Nd}_2\text{O}_3)_{0.2}$  and  $(\text{Bi}_2\text{O}_3)_{0.5}(\text{Nd}_2\text{O}_3)_{0.5}$  present more complex diffraction patterns. The former seems to consist of a two-phase mixture in the investigated temperature range. Fig. 1b shows the diffraction pattern of the sample treated at 900°C and quenched in air. Diffraction maxima can be observed corresponding to an f.c.c.  $\delta\text{-Bi}_2\text{O}_3$  phase, together with additional maxima which can be assigned to a Bi–Sr–O-type structure with rhombohedral symmetry [8] (JCPDS card 41-0310). When the sample is quenched in liquid nitrogen from 900°C the proportion of the cubic phase is higher. However, when the sample is slowly cooled from 900°C to room temperature or when the annealing temperature is increased, the proportion of this cubic phase decreases. In this sense, although the rhombohedral phase has not been obtained as a pure phase, the reflection maxima corresponding to the f.c.c. phase appear with a very low intensity in the diffraction pattern of the sample heated at 1100°C.

On the other hand, the diffraction pattern of

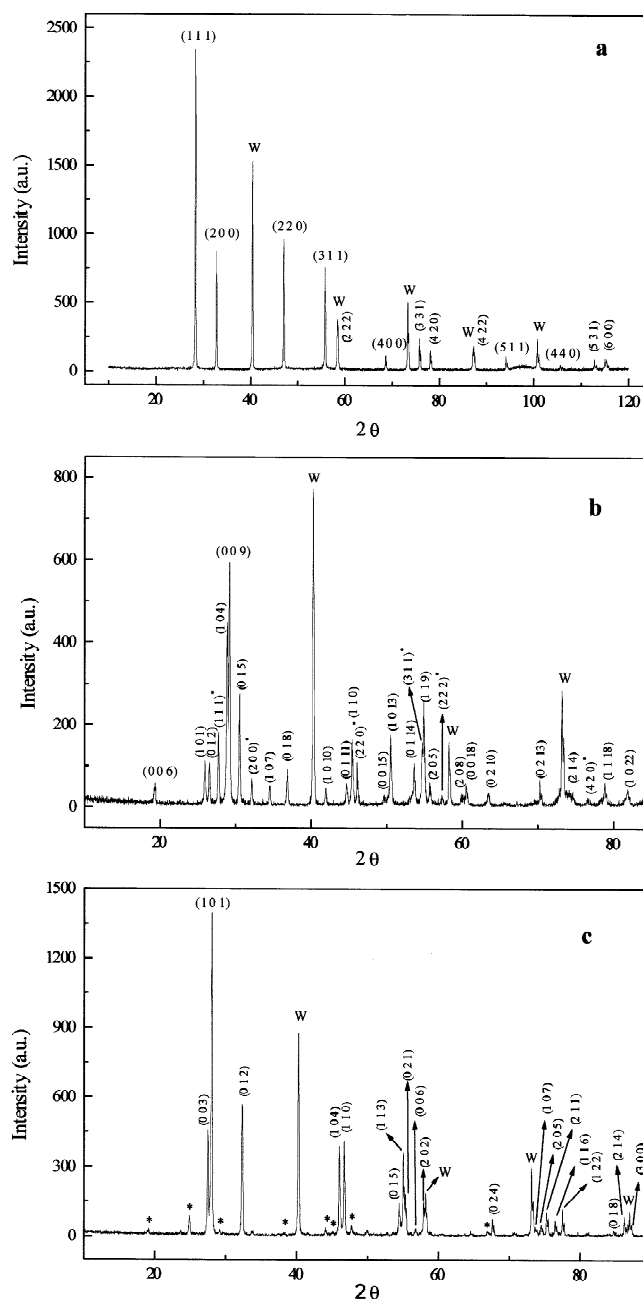


Fig. 1. X-ray diffraction patterns obtained for: (a)  $(\text{Bi}_2\text{O}_3)_{0.65}(\text{Dy}_2\text{O}_3)_{0.35}$  sample annealed at 900°C; (b)  $(\text{Bi}_2\text{O}_3)_{0.8}(\text{Nd}_2\text{O}_3)_{0.2}$  sample annealed at 900°C and quenched in air; Miller indices marked with an asterisk correspond to the f.c.c. phase (see text); and (c)  $(\text{Bi}_2\text{O}_3)_{0.5}(\text{Nd}_2\text{O}_3)_{0.5}$  sample annealed at 1200°C; diffraction maxima marked with an asterisk are due to a superstructure (see text).

$(\text{Bi}_2\text{O}_3)_{0.5}(\text{Nd}_2\text{O}_3)_{0.5}$  sample treated at 1200°C (Fig. 1c) shows high intensity maxima which can be indexed in the rhombohedral unit cell of the  $\text{Bi}_3\text{R}_5\text{O}_{12}$ -type structure [9]. Very weak diffraction lines probably due to a superstructure  $8a \times 2c$  are also observed [9] (JCPDS card 47-0300). This result could be understood considering the loss of  $\text{Bi}_2\text{O}_3$  oxide that takes place at high temperature. The composition  $(\text{Bi}_2\text{O}_3)_{0.37}(\text{Nd}_2\text{O}_3)_{0.63}$  obtained from

Table 1  
Room temperature lattice parameters of the synthesized pure  $(\text{Bi}_2\text{O}_3)_{1-x}(\text{R}_2\text{O}_3)_x$  phases

| Compound <sup>a</sup>  | Lattice parameters (Å)        |
|--|-------------------------------|
| $(\text{Bi}_2\text{O}_3)_{0.6}(\text{Sm}_2\text{O}_3)_{0.4}$   | 5.5198(3)                     |
| $(\text{Bi}_2\text{O}_3)_{0.65}(\text{Dy}_2\text{O}_3)_{0.35}$ | 5.4725(2)                     |
| $(\text{Bi}_2\text{O}_3)_{0.5}(\text{Nd}_2\text{O}_3)_{0.5}$   | $a=3.8844(3)$<br>$c=9.712(2)$ |

<sup>a</sup> Nominal composition.

semiquantitative EDS analyses confirms this assumption. The calculated rhombohedral subcell parameters are given in Table 1. In the case of the samples obtained at temperatures lower than 1200°C the oxide seems to consist of a mixture of two phases with rhombohedral symmetry. The majority phase is the previously indicated  $\text{Bi}_3\text{R}_5\text{O}_{12}$ -type and the second one, which presents the Bi–Sr–O-type structure, corresponds to the solid solution  $\text{Bi}_{1-x}\text{Nd}_x\text{O}_{1.5}$  in the Bi-rich side.

Diffuse reflectance data corresponding to the  $(\text{Bi}_2\text{O}_3)_{0.6}(\text{Sm}_2\text{O}_3)_{0.4}$  and  $(\text{Bi}_2\text{O}_3)_{0.65}(\text{Dy}_2\text{O}_3)_{0.35}$  samples treated at 1000°C and  $(\text{Bi}_2\text{O}_3)_{0.5}(\text{Nd}_2\text{O}_3)_{0.5}$  sample treated

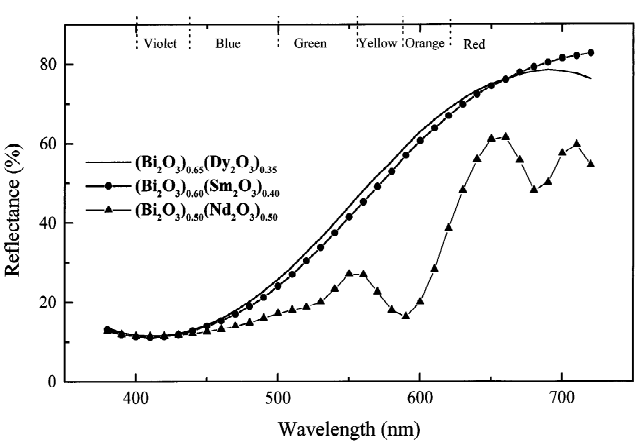


Fig. 3. Reflectance spectra for  $(\text{Bi}_2\text{O}_3)_{0.6}(\text{Sm}_2\text{O}_3)_{0.4}$ ,  $(\text{Bi}_2\text{O}_3)_{0.65}(\text{Dy}_2\text{O}_3)_{0.35}$  and  $(\text{Bi}_2\text{O}_3)_{0.5}(\text{Nd}_2\text{O}_3)_{0.5}$  samples.

at 1200°C, are shown in Fig. 3. The obtained CIE-LAB color coordinates of these three samples are collected in Table 2. As can be observed, in the case of the samarium and dysprosium samples the reflectance curves show broad absorption bands for  $\lambda \leq 500$  nm and reflection bands for

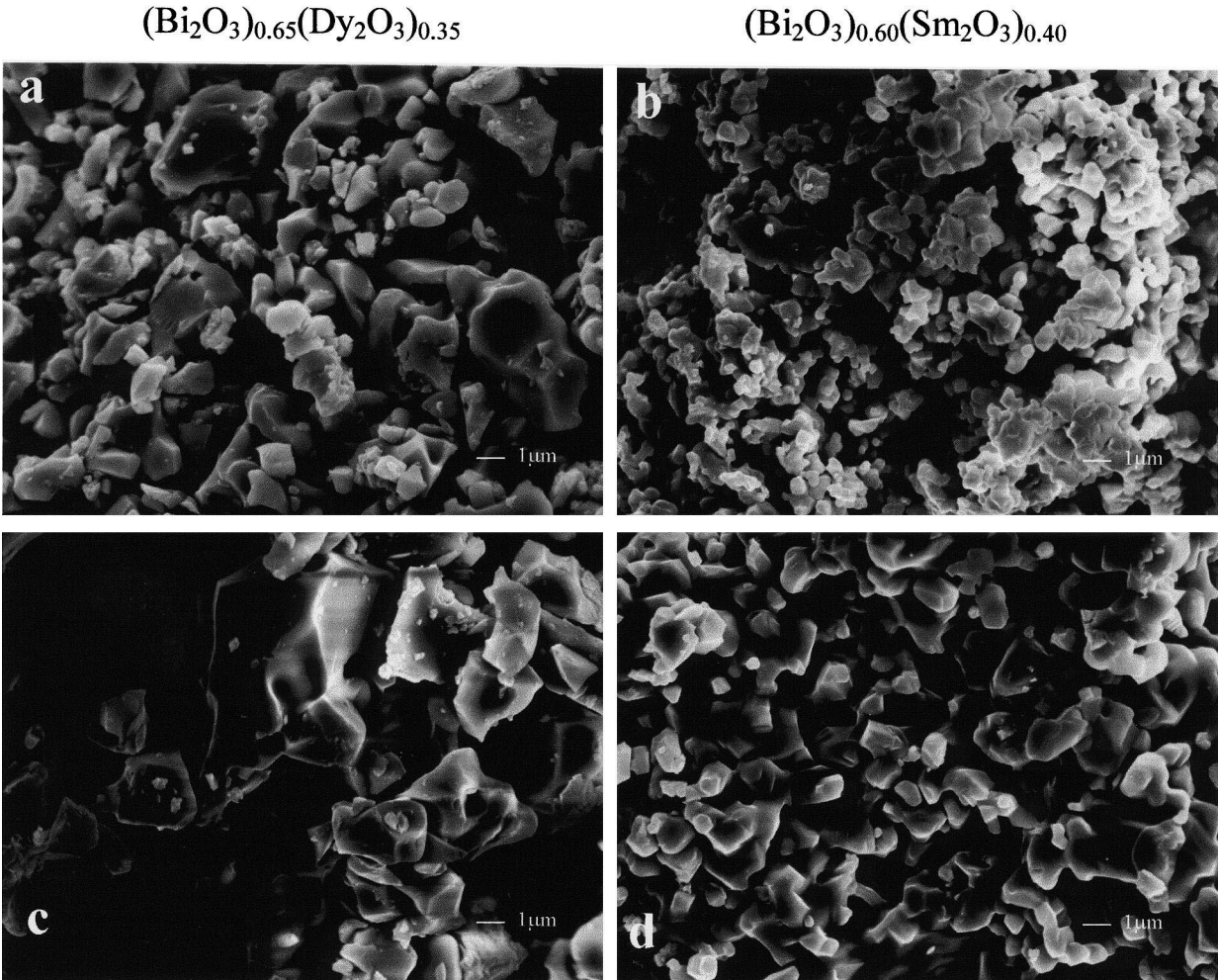


Fig. 2. Scanning electron micrographs of  $(\text{Bi}_2\text{O}_3)_{0.6}(\text{Sm}_2\text{O}_3)_{0.4}$  and  $(\text{Bi}_2\text{O}_3)_{0.65}(\text{Dy}_2\text{O}_3)_{0.35}$  samples annealed at 900 (a and b) and 1000°C (c and d).

Table 2

Color parameters and reflection percentage ( $R$ ) of the obtained pure  $(\text{Bi}_2\text{O}_3)_{1-x}(\text{R}_2\text{O}_3)_x$  phases

| Compound <sup>a</sup>   | $L^*$ | $a^*$ | $b^*$ | $C^*$ | $R_{400}$ (%) | $R_{700}$ (%) |
|---|-------|-------|-------|-------|---------------|---------------|
| $(\text{Bi}_2\text{O}_3)_{0.6}(\text{Sm}_2\text{O}_3)_{0.4}$ <sup>b</sup>   | 71.21 | 16.30 | 43.98 | 46.91 | 11.44         | 81.43         |
| $(\text{Bi}_2\text{O}_3)_{0.65}(\text{Dy}_2\text{O}_3)_{0.35}$ <sup>b</sup> | 72.69 | 14.89 | 45.21 | 47.60 | 11.89         | 78.23         |
| $(\text{Bi}_2\text{O}_3)_{0.5}(\text{Nd}_2\text{O}_3)_{0.5}$ <sup>c</sup>   | 55.09 | 10.20 | 20.88 | 23.24 | 11.64         | 57.47         |

<sup>a</sup> Nominal composition.<sup>b</sup> Samples annealed at 1000°C.<sup>c</sup> Sample annealed at 1200°C.

higher wavelengths with a steep slope from 500 to 650 nm. These samples present a strong yellow component (low  $a^*$  and high  $b^*$  values) and very high lightness ( $L^*$ ) (Table 2). The reflectance spectra of the neodymium sample shows absorption bands in the 450–700-nm range, which can be assigned to the intra-atomic  $4f-4f$  transitions. The reflection percentage in the high wavelength region ( $R_{700}$ ) is lower than the  $R_{700}$  values of dysprosium and samarium samples, as can be observed in Table 2. The obtained values of the lightness, purity of the color ( $C^*$ ) and reflection percentage  $R_{700}$ , suggest that the  $(\text{Bi}_2\text{O}_3)_{0.6}(\text{Sm}_2\text{O}_3)_{0.4}$  and  $(\text{Bi}_2\text{O}_3)_{0.65}(\text{Dy}_2\text{O}_3)_{0.35}$  oxides can be used as inorganic pigments.

### Acknowledgements

The authors thank the CICYT for financial support under Project MAT97-0697 and Rhodia Terres Rares for

provide chemical reactants and discussions. We also thank the Centro de Microscopía Electrónica of the UCM for technical support.

### References

- [1] T. Takahashi, H. Iwahara, Y. Nagai, J. Electrochem. 2 (1972) 97.
- [2] H.A. Harwing, Z. Anorg. Allg. Chem. 444 (1978) 151.
- [3] T. Takahashi, H. Iwahara, Mater. Res. Bull. 13 (1978) 1447.
- [4] H. Iwahara, T. Esaka, T. Sato, T. Takahashi, J. Solid State Chem. 39 (1981) 173.
- [5] A. Watanabe, J. Solid State Chem. 120 (1995) 32.
- [6] A. Watanabe, J. Solid State Chem. 124 (1996) 287.
- [7] M. Drache, P. Conflant, S. Obbade, J.P. Wignacourt, A. Watanabe, J. Solid State Chem. 129 (1997) 98.
- [8] M. Drache, S. Obbade, J.P. Wignacourt, P. Conflant, J. Solid State Chem. 142 (1999) 349.
- [9] R. Horyn, M. Wolcyrz, A. Wojakowski, J. Solid State Chem. 116 (1995) 68.